New Member-Set (P21^e) of TEAM Problem 21 Family for Modeling and Validation of Stray-Field Loss under Harmonics and DC Hybrid Excitation

Zhiguang Cheng[1], Behzad Forghani[2], Zhenbin Du[1], Lanrong Liu[1], Yongjian Li[3], and Xiaojun Zhao[4]

[1]Institute of Power Transmission and Transformation Technology, Baobian Electric, Baoding, China
[2]Mentor Infolytica, a Siemens Business, Montreal, Canada
[3]State Key Laboratory of Reliability and Intelligence of Electrical Equipment, Hebei University of Technology, Tianjin, China
[4]Dept. of Electrical Engineering, North China Electric Power University, Baoding, China
E-mails: [1] emlab@btw.cn, [2]behzad.forghani@siemens.com, [3]liyongjian@hebut.edu.cn,[4] zxjncepu@ncepu.edu.cn

TEAM Problem 21, an engineering-oriented loss model, was proposed in 1993, and its benchmark family of 16 member models was well established in 2009 following three updates (in 1999, 2005, and 2009). The measured and calculated results of these benchmark models have been presented worldwide. Note that in the previous version of TEAM Problem 21, all the magnetic or non-magnetic load-components of member-models are excited by sinusoidal currents (50Hz). However, new requirements and challenges have been arising in increasing the effectiveness and usefulness of large-scale modeling and simulation under complex excitation conditions. To confidently model and validate the stray-field loss in the models' load-components under non-sinusoidal excitation, additional updates to Problem 21 Family are proposed, as its new member-set(P21^e), including the enhanced excitation setup with magnetic flux compensation, the enlarged models' load-components with updated material, and the measurements of materials' electric and magnetic properties under complex excitations.

In the upgraded models, the typical magnetic or non-magnetic load-components (GO silicon steel sheets and copper plate) are excited by sources containing harmonics and DC using a hybrid power supply rather than sinusoidal excitation, as in the previous version of the TEAM Problem 21 Family. All the new extensions will be beneficial to the high-performance benchmarking and industrial application.

***Index Terms*: New member-set, benchmark family, exciting coils and compensating coils, load-component, silicon steel lamination, copper plate, magnetic flux, stray-field loss, additional loss, non-sinusoidal excitation (NSE), harmonics & DC-bias, electric and magnetic property, magnetic flux compensation.**

I. INTRODUCTION

As one of the ICS (International Compumag Society) benchmark problems, the TEAM Problem 21 was proposed in 1993 based on the industrial background of modeling stray-field loss in electrical equipment. Since then, it has been extended to a TEAM Benchmark Family, including five sets of 16 member-models, approved by the ICS in 2009[1-16].

There is a broad consensus that the effectiveness of computational electromagnetic modeling and simulation depends not only on efficient electromagnetic analysis methods and computational software but also on sufficient and applicable material property data. Consequently, the accurate measurement and prediction of material's electromagnetic properties under complex and even extreme working conditions are essential for reliable numerical analysis, especially for the growing demand in industrial applications. Therefore, the highly developed benchmarking (TEAM) research in computational electromagnetics, proposed and strongly advocated by the ICS, would be further extended and promoted instead of staying in the past. The new benchmark models to be established will also contain essential scientific connotations and industrial background, even involving coupled multi-physics field modeling and validation, to further meet the growing requirements in the science and engineering-related fields.

This benchmarking report very briefly outlines the essential characteristics and the upgrades to the TEAM Problem 21 Family (since 1993), refers to its V.2009 in detail [16], and emphasizes the combination of high-performance analysis methods with advanced material property modeling. For an in-depth investigation of the stray-field loss under non-sinusoidal excitations, a new member-set (P21^e) of Problem 21 Family is proposed. In the new member-set, the typical magnetic and non-magnetic load-components of the two upgraded member models are excited by sources containing harmonics and DC. The choice of the new member models is based on the relevant research works that have been done recently by our co-research group [17-24]. Here, the definition of the new member-set (P21^e), including all the input data, the measuring system, and the typical benchmarking results, are presented.

II. NEW UPDATES OF PROBLEM 21 FAMILY

2.1 Upgraded Models

To realize AC-DC hybrid excitation and to enhance the excitation supply, the original exciting coils of Problem 21 Family (V.2009) have been upgraded as follows:

(1) The number of turns of each exciting coil is increased from 300 to 400, and the coil copper-wire dimension is upgraded from 6.7×2.0 mm to 9.0×3.0 mm (thus, the net wire sectional area is increased to 26.45mm^2). In addition, the dimensions of the magnetic and non-magnetic load-

components (i.e., GO silicon steel lamination and copper plate） are increased compared to that of the related member-models in V.2009, and the materials of those load-components are changed as well.

(2) Two compensating coils (C-coil 1 and C-coil 2 used for magnetic flux compensation of E-coils) are configured to keep the leakage magnetic field of the exciting coils almost the same when the model's load-component (e.g., GO (grain-oriented) silicon steel lamination or copper plate) is removed (referred to as the no-load case), thus keeping the loss generated in the exciting coils almost the same. The effectiveness of magnetic flux compensation by using C-coils has been demonstrated [19-20].

The compensating coils have the same specifications as the exciting coils (E-coils). See Fig.1(a). The two compensating coils are movable on parallel rails to adjust the C-coils' positions easily, as shown in Fig.1 (b).

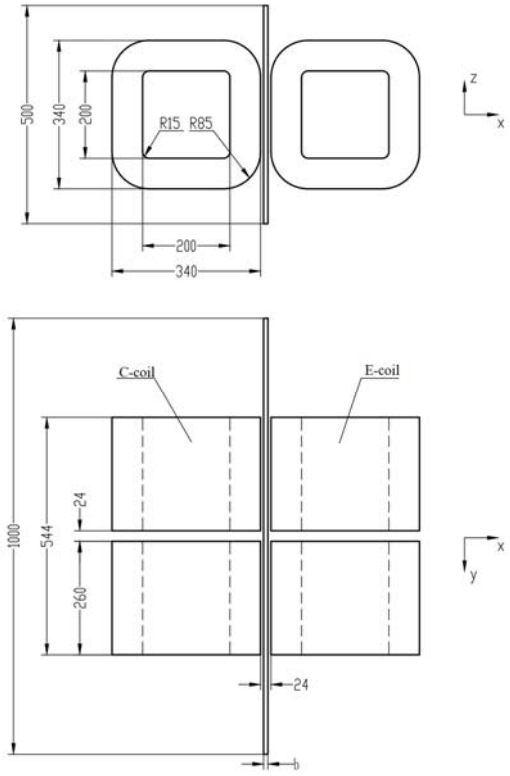

(a) Exciting & compensating coils with model's load-component

Note: Here *b* denotes the thickness of different model's load-component: *b*=6mm (copper plate) for Model P21^e-EM(NS); and *b*=6.6mm (laminated sheets) for Model P21^e-M(NS).

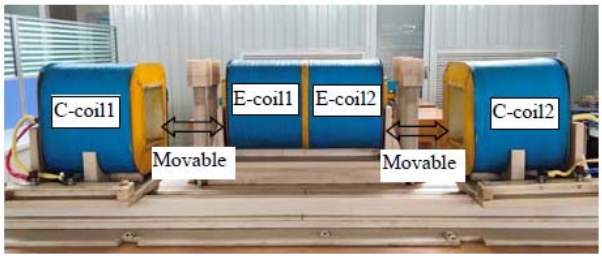

(b) Exciting and compensating system

Fig.1 Upgraded exciting & compensating setup of Problem 21 Family

Note that the excitation direction of E-coil 1 and E-coil 2 in the upgraded models can be selected to be the opposite (Pattern I) or the same (Pattern II). Of course, the results of measurement or calculation will be different with a different choice. In this benchmarking report, Pattern I is selected in both measurement and numerical simulation.

2.2 Extended TEAM Problem 21 Family

Based on the original member models P21^c-EM1, and P21^d-M, a new member-set (P21^e) of the Problem 21 Family is formed with AC-DC hybrid excitation, i.e., P21^e-EM (NS) and P21^e-M(NS), where NS denotes non-sinusoidal excitation. In the current extended version of TEAM Problem 21 Family, two upgraded member-models have been established as its new member-set. So the Problem 21 Family now includes six sets of 18 member models, as shown in Table I.

Table I
Extended Problem 21 Family (2021)

Member set	Models	Problem features	Proposed at
Problem 21 Family (V.2009)			
P21^0	P21^0-A P21^0-B	3-D nonlinear eddy current and hysteresis model with multiply connected regions (sinusoidal excitation).	TEAM-Miami, USA, 1993[1].
P21^a	P21^a-0 P21^a-1 P21^a-2 P21^a-3	3-D linear eddy current model with multiply connected regions (sinusoidal excitation).	TEAM-Yichang, China, 1996[2].
P21^b	P21^b-MN P21^b-2M P21^b-2N	3-D nonlinear eddy current and hysteresis model with magnetic or/and non-magnetic steel plates separately placed (sinusoidal excitation).	IEE CEM, Bournemouth, UK, 2002[6].
	P21^b-MNM P21^b-NMN	3-D nonlinear eddy current and hysteresis model with magnetic and non-magnetic steel plates welded together (sinusoidal excitation).	ACES, Miami, USA, 2006[10].
P21^c	P21^c-M1 P21^c-M2 P21^c-EM1 P21^c-EM2	Magnetic shielding and electromagnetic shielding models: 3-D nonlinear eddy current and hysteresis model with anisotropic lamination (sinusoidal excitation)	Compumag, Shenyang, China, 2005[8].
P21^d	P21^d-M	3-D nonlinear eddy current and hysteresis model with anisotropic lamination without solid magnetic steel (sinusoidal excitation).	IEEE CEFC-Athens, Greece, 2008[13-15].
New member-set of TEAM Problem 21 Family			
P21^e	P21^e-EM(NS)	3-D linear eddy current model with non-sinusoidal excitation	1& 2DM, Tianjin, China, 2016[21, 24]
	P21^e-M(NS)	3-D nonlinear/anisotropic eddy current and hysteresis model with non-sinusoidal excitation	

The descriptions of the main specification parameters of the upgraded models' load-components can be seen in Table II.

Table II
Upgraded Models' Load-components

Models	Material	Dimensions(mm)	Amount
P21^e-EM(NS)	Copper plate (T2Y)	1000×500×6	1
P21^e-M(NS)	GO silicon steel sheets (B27R090, Baosteel)	1000×500×0.27	24

2.3 Benchmarking Targets and Input Data of P21^e

2.3.1 Benchmarking Target for New member-set (P21^e)

(a) Defined numerical Analysis and Measurement of P21^e

The benchmarking targets of the new member-set (P21^e-EM(NS) and P21^e-M(NS)) of Problem 21 Family are defined as follows:

1) The numerical analysis and the measurement of the stray-field losses inside magnetic and non-magnetic load-components of the upgraded models(P21^e) under prescribed non-sinusoidal excitations (NSE), as given in Table III.

2) The numerical analysis and the measurement of the magnetic flux densities at the indicated positions (shown in Table VI and Table VII) under prescribed NSE conditions.

(b) Computation Notes

1) The new member-set (P21^e) has to be solved using a transient solver due to the harmonics and DC hybrid excitation. It is computationally challenging, but achievable. The complete material properties and exciting current waveforms under prescribed NSE conditions are provided in the attached input data files, as described in 2.3.2.

2) The eddy current loss caused by leakage magnetic flux perpendicular to the laminations (B_x) in P21^e-M(NS) must be handled carefully, which is not included in the magnetic loss measured by 1-D or 2-D magnetic measuring system. Thus it is referred to as an additional loss, P_a, which can be calculated using (1)[24],

$$P_a = \int_\Omega \frac{\left|\boldsymbol{J}_{yz}\right|^2}{[\sigma]} dv \tag{1}$$

where $\boldsymbol{J}_{yz}$ denotes the induced 2-D eddy currents in laminated sheets by magnetic flux (B_x) perpendicular to laminations. To numerically determine the additional loss P_a, as one of the prediction schemes, the normal component(σ_x) of the conductivity of GO silicon steel sheet ([σ]) is forced to zero to include the eddy current loss caused by the normal flux only, as shown in (2),

$$[\sigma] = \begin{bmatrix} 0 & & \\ & \sigma_y & \\ & & \sigma_z \end{bmatrix} \tag{2}$$

Considering the additional loss discussed above, the total loss inside the laminated sheets (P21^e-M (NS)) under non-sinusoidal excitation, P_{tm}, consists of two parts; one part is generated by the main magnetic flux (at NSE condition) inside the laminated sheets, namely $P_{m(nse)}$, and the other part is generated by the leakage magnetic flux perpendicular to the laminations, namely P_a, so P_{tm} can be determined by (3)

$$\begin{aligned} P_{tm} &= P_{m(nse)} + P_a \\ &= \int_\Omega W_{m(nse)} dv + \int_\Omega \frac{\left|J_{yz}\right|^2}{[\sigma]} dv \end{aligned} \tag{3}$$

where $W_{m(nse)}$ is the specific total magnetic loss, depending on the measured magnetic loss property and the calculated magnetic flux density under NSE condition.

2.3.2 Input Data for New member-set (P21^e)

The input data used for numerical simulation of the new member set (P21^e) under all the defined non-sinusoidal excitations are attached to this benchmark report, including:

1) Model design parameters and material electric properties (P21^e);
2) Measured magnetic properties of GO silicon steel (B27R090, Baosteel, used in P21^e-M(NS));
3) Measured exciting current waveforms of all excitation cases (Case I -V, P21^e).

2.4 Harmonics and DC Hybrid Excitation

(a) AC-DC Hybrid Excitation System

The AC-DC hybrid excitation system consists of a 30MHz multi-function generator (NF), three sets of precision power amplifier 4520A & power booster 4521A(NF), Precision power analyzer WT3000E (Yokogawa), DC supply, and the upgraded benchmark models, as shown in Fig.2.

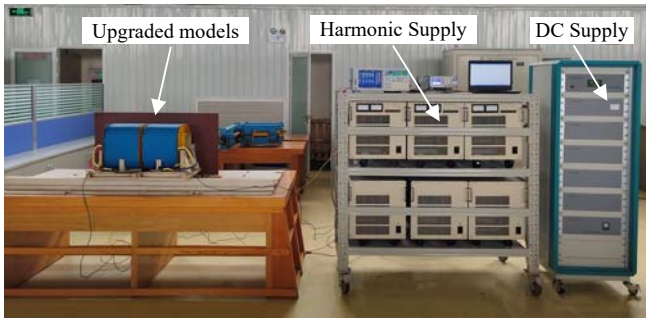

Fig.2 Measuring system with AC-DC hybrid excitation and upgraded model

Note that two modes, CV/AC and CV/DC (here CV denotes constant voltage) of the Power Amplifier (4520A, NF), can be selected. In the CV/AC mode, the voltage-source excitation includes fundamental and harmonic components. In contrast, in the CV/DC mode, the voltage-source excitation can also include DC components, as well as fundamental and harmonic components.

(b) Two Hybrid Excitation Modes

Based on the measuring system shown in Fig.2, two AC-DC hybrid excitation modes are realized:

One is to apply AC and DC on the same side of the

model's load-component, i.e., mode 1 of AC-DC hybrid excitation, represented by ADH1, as shown in Fig.3.

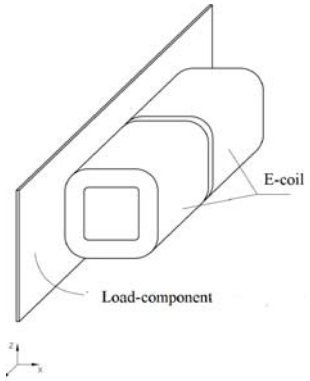

Fig.3 One-side excitation (ADH1)

Another one is to apply AC and DC on the two sides of the model's load-component, i.e., mode 2 of AC-DC hybrid excitation, represented by ADH2, as shown in Fig.4.

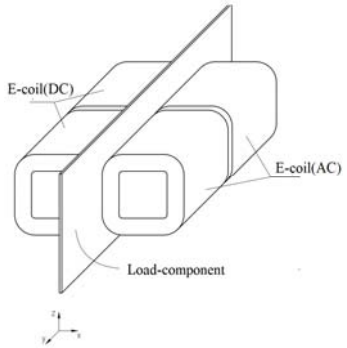

Fig.4 Two side excitation (ADH2)

All the AC-DC hybrid excitation cases based on the upgraded models of the new member-set of Problem 21 Family (P21^c-EM(NS) and P21^c-M(NS)) are specified, as shown in Table III.

Table III
AC-DC Hybrid Excitation Cases

Cases	Excitation conditions	
I	$U_1 \sin(\omega t+0)$	In each case, the excitation current (AC) reaches 10A (rms), but without DC component.
II	$U_1 \sin(\omega t+0)+U_3 \sin(3\omega t+0)$	
III	$U_1 \sin(\omega t+0)+U_3 \sin(3\omega t+0)+U_5 \sin(5\omega t+0)+U_7 \sin(7\omega t+0)$	
IV (ADH1)	$U_1 \sin(\omega t+0)+U_3 \sin(3\omega t+0)$ *(with DC component)*	Hybrid excitation at the same side of model's load-component, AC reaches 7A (rms), and includes DC (5A).
V (ADH2)	$U_1 \sin(\omega t+0)+U_3 \sin(3\omega t+0)$ *(with DC component)*	Hybrid excitation at the two side of model's load-component, AC reaches 7A (rms) at one side, and DC reaches 5A at another side.

Notes:
All phase angles of fundamental and harmonics are set to zero. U_1 (fundamental, 50Hz, rms); U_3, U_5, and U_7 are of 30% U_1.

III. Loss Prediction under AC-DC Hybrid Excitation

The measured total on-load loss P_t includes the loss in the model's load-component, P_x, and the loss in all the exciting coils under AC-DC hybrid excitation condition (P_{Ecoils}).

3.1 In the Case of One-Side Excitation (ADH1)

To determine the E-coils' loss, remove the square load-component from the assembled model shown in Fig.3 (ADH1) and place the two C-coils, as shown in Fig.5. After that, the same exciting currents (i.e., equal to the exciting currents under on-load condition) are applied to exciting coils and compensating coils, then the loss in E-coils (P_{Ecoils}) can be measured. P_x can be determined using (4)

$$P_x = P_t - P_{Ecoils} \tag{4}$$

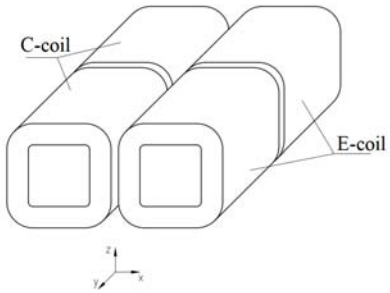

Fig.5 No-load case (with magnetic flux compensation)

3.2 In the Case of Two-Side Excitation (ADH2)

In the case of two-side excitation (ADH2), the C-coils are used as the DC supply, as shown in Fig.4. Similar to the method described in 3.1 above, the losses in both E-coils and C-coils, P_{Ecoils} and P_{Ccoils}, can be determined. Then P_x can be obtained using (5),

$$P_x = P_t - (P_{Ecoils} + P_{Ccoils}) \tag{5}$$

It should be noted that in magnetic flux compensation (with the no-load condition), the excitation direction of the compensation coil will be different for the magnetic and non-magnetic load-components used in the upgraded model.

In addition, the stray-field loss in the model's load-component P_x can be determined based on the measured total loss (P_t) and the calculated exciting coils' loss $P_{cal(Ecoils)}$, as shown in (6),

$$P_x = P_t - P_{cal(Ecoils)} \tag{6}$$

Comparing all the loss results using different methods helps validate numerical analysis and material modeling, especially under complex excitations.

Conclusively, the upgraded benchmark models enable us to realize the harmonics-DC hybrid excitation and determine the stray-field loss inside the model's load-component based on the measured results, obtained from both on-load (with load-component) and no-load (without load-component, but using

compensating coils) cases. This is beneficial for a reliable evaluation of the stray-field loss in the model's load-component.

IV. Benchmarking Results Based on P21^e Models

In this benchmarking report, the stray-field loss inside magnetic and non-magnetic load-components of each upgraded model has been calculated and measured under different harmonic and DC hybrid excitation conditions. In addition, the magnetic flux densities at some specified positions are also calculated and measured.

Note that all phase angles of fundamental and harmonics are set to zero for highlighting the basic field characteristics and the key problems to be solved under harmonics and DC hybrid excitations, with possible simplicity.

4.1 Stray-field Losses in Models' Load-components

The calculated and measured stray-field losses inside the copper plate of P21^e-EM(NS), under sinusoidal and non-sinusoidal excitations (with different harmonic and DC components), such as Cases I-V (see Table III), are shown in Table IV.

Table IV
Stray-field Loss in Copper Plate (P21^e-EM(NS))

Cases	On-load loss (W)	No-load loss with magnetic flux compensation (W)	Loss in load-components (W)	
			Based on both on-load and no-load loss results	Calculated
I	85.51	66.15	19.36	19.072
II	86.69	67.21	19.48	19.127
III	88.99	69.39	19.60	19.225
IV (ADH1)	54.88	45.38	9.50	9.321
V (ADH2)	53.96	45.44	8.52	8.425

Fig.6 shows the comparison between the calculated and measured stray-field losses inside the load-component (copper plate) under different excitations (Cases I-V).

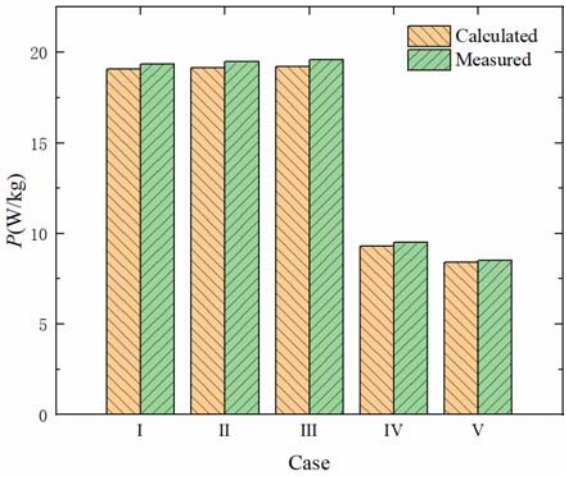

Fig.6 Comparison between calculated and measured loss results in copper plate under different excitations (P21^e-EM(NS))

The calculated and measured stray-field losses inside the GO silicon steel lamination of P21^e-M(NS), under sinusoidal and non-sinusoidal excitations (with different harmonic and DC components), such as Cases I-V (see Table III), are shown in Table V and Fig.7. Where $P_{m(nse)}$, P_a, denote total magnetic loss and additional loss inside load-component, respectively, See (3) for details.

Table V
Stray-field Loss in GO Silicon Steel Lamination (P21^e-M(NS))

Cases	On-load loss (W)	No-load loss with magnetic flux compen-sation (W)	Loss in load-components (W)			
			Based on both the on-load and no-load loss results	Calculated		
				$P_{m(nse)}$	P_a	P_{tm} $(P_{m(nse)}+P_a)$
I	76.29	70.52	5.77	1.463	4.167	5.630
II	78.42	72.03	6.39	1.551	4.488	6.039
III	82.42	74.96	7.46	1.953	5.683	7.636
IV (ADH1)	50.37	47.57	2.80	0.842	1.876	2.718
V (ADH2)	50.29	47.79	2.50	0.741	1.821	2.562

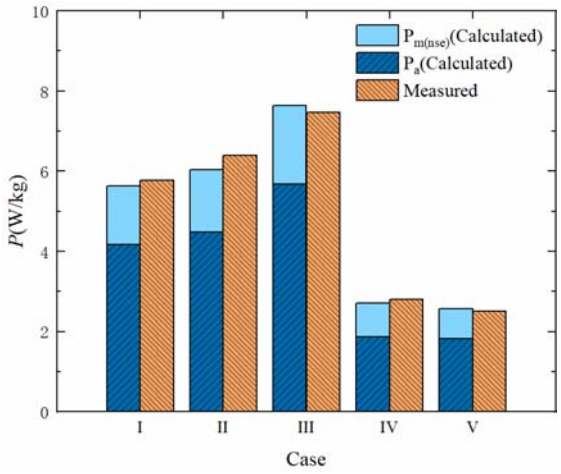

Fig.7 Comparison between calculated and measured loss results in GO silicon steel laminations under different excitations (P21^e-M(NS))

4.2 Magnetic Flux Densities at Specified Positions

The magnetic flux densities at the specified positions, i.e., at the side facing E-coils, have been calculated and measured based on P21^e-EM(NS) and P21^e-M(NS) under specified excitation conditions (Cases I-IV).

As an example of typical multi-harmonic excitation (Case III, including fundamental, and 3rd, 5th and 7th harmonics), the measured and calculated results of magnetic flux densities (B_x) are shown in Table VI for model P21^e-EM(NS) and in Table VII for model P21^e-M(NS), respectively.

Table VI
Calculated and Measured Magnetic Flux Density B_x($\times 10^{-4}$T)
(P21^e-EM(NS): Case III)

Z (mm)	y=0, x=-3-δ(mm)		y=278, x=-3-δ(mm)	
	Meas.	Calc.	Meas.	Calc.
0	19.75	24.91	11.84	13.52
25.0	19.51	24.54	12.17	13.11
50.0	19.70	26.40	11.36	13.71
75.0	17.88	23.19	10.11	12.86

100.0	14.57	19.51	7.42	10.27
125.0	10.37	13.73	4.66	6.70
150.0	6.75	8.70	2.30	3.53
175.0	4.98	5.40	1.15	1.63
200.0	5.75	5.74	0.87	1.35
225.0	11.46	10.43	2.01	2.79
250.0	45.68	40.15	11.62	9.22

Table VII
Calculated and Measured Magnetic Flux Density B_x($\times 10^{-4}$T)
(P21^e-M(NS): Case III)

Z (mm)	y=0, x=-3-δ(mm)		y=278, x=-3-δ(mm)	
	Meas.	Calc.	Meas.	Calc.
0	154.07	165.15	82.34	77.09
25.0	153.97	162.10	81.06	79.19
50.0	147.97	155.24	77.55	78.31
75.0	137.05	144.41	70.43	74.15
100.0	116.82	128.10	57.75	62.52
125.0	91.87	99.09	43.56	46.71
150.0	69.11	72.82	30.49	33.09
175.0	49.36	52.20	21.18	23.07
200.0	36.43	37.56	14.45	14.85
225.0	28.33	30.32	10.41	11.14
250.0	34.46	33.75	12.31	12.18

The Gauss/Teslameter (Model 7010) is used in this measurement of magnetic flux densities. To correctly determine the positions for measuring or calculating magnetic flux densities, the probe's 1/2 thickness δ(i.e., δ=0.76mm) shall be taken into account because the measuring point of magnetic flux density is located in the center of the Gaussmeter probe in thickness.

Fig.8 shows the comparisons between calculated and measured results of magnetic flux densities at the specified positions for model P21^e-EM(NS) and P21^e-M(NS), respectively.

It should be pointed out that the upgraded model P21^e-M(NS) enables us to examine the nonuniformity of magnetic flux and stray field loss in detail at the single sheet level.

Fig. 9 shows the magnetic flux distributions in different layers of laminated sheets in P21^e-M(NS) under multi-harmonic excitation, as in Case III.

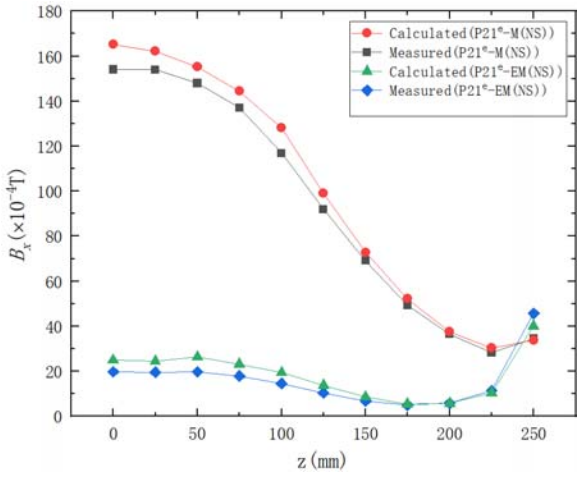

(a) y=0mm

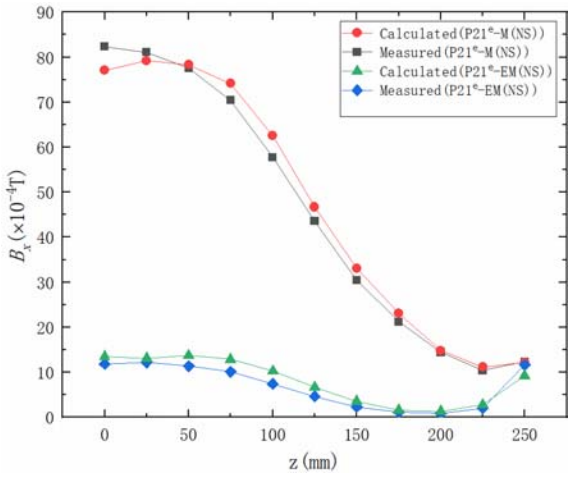

(b) y=278mm

Fig.8 Calculated and Measured Magnetic Flux Densities(B_x)
(P21^e-M(NS)/EM(NS): Case III)

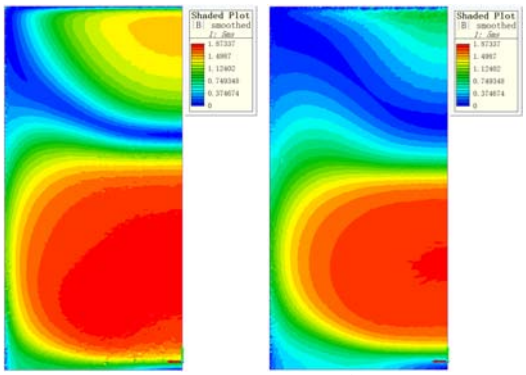
(a) 1st sheet (b) 2nd sheet

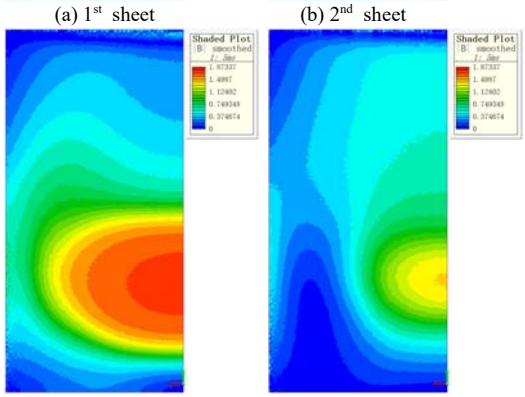
(c) 3rd sheet (d) 4th sheet

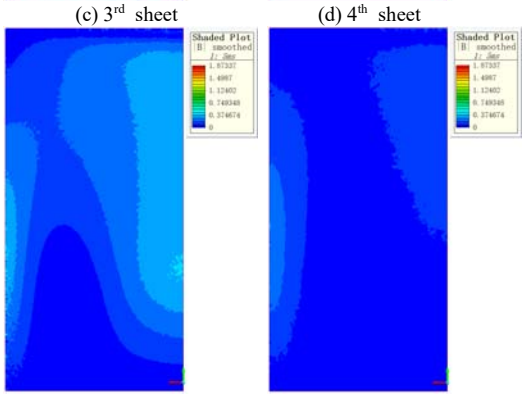
(e) 5th sheet (f) Equivalent bulk part

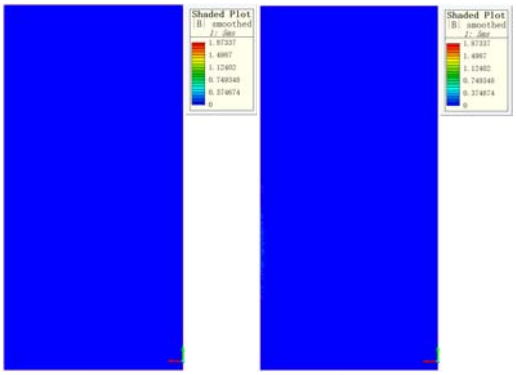

(g) 23rd sheet (h) 24th sheet

Fig.9 Magnetic flux distributions at different layers(P21^e-M(NS), Case III)

In Fig.9 the sequence of the layers starts with the first sheet where the magnetic flux entered. Refer to Fig.3.

Note that the simulation results shown in Tables IV-VII and Figs.6-9 are obtained by using Simcenter^{TM} MAGNET^{TM} software.

V. Benchmarking Remarks

To meet the increasing requirements for effective modeling and simulation, especially under complex non-sinusoidal excitations, the new member-set (P21^e) of TEAM Problem 21 Family has been created, based on the recent extended benchmarking (TEAM) done by our co-research group, and following the helpful comments from colleagues in computational electromagnetics.

According to the new member-set(P21^e) definition, the calculated and measured results of both stray-field loss and magnetic flux densities have been obtained at the different excitations, using Simcenter^{TM} MAGNET^{TM} software and the well-established measuring system. All the benchmarking results show that:

1) The non-sinusoidal excitation, with harmonics and DC components, has been realized. The new benchmarking results, under harmonics and DC hybrid excitations, based on the new member-set of TEAM Problem 21 Family, have been presented in this report to show the different loss behaviors of magnetic and non-magnetic load-components under different excitations.

2) The upgraded benchmark models with magnetic flux compensation enable us to determine the stray-field loss inside the model's load-component based on the measured results, obtained from both on-load (with load-component) and no-load (without load-component, but using compensating coils) cases.

3) The measurement and calculation results (of stray-field losses inside load-components and leakage flux densities at prescribed positions) obtained from the new member-set of Problem 21 Family are practically in good agreement, demonstrating the effectiveness of the numerical simulation, the material property measurement, and the magnetic flux compensation, under all excitation conditions.

4) It is certainly expected to have more improved results concerning the new member-set of Problem 21 Family(P21^e), presented by colleagues worldwide, using various efficient and practical solvers, pushing forward future benchmarking and industrial application.

Acknowledgements

All colleagues of our international co-research group would like to extend their deep gratitude to Prof. D. Lowther, Prof. J. Sykulski, and the ICS Board for approving the new updates of the Problem 21 Benchmark Family, to all supporters and collaborators, including Prof. Dexin Xie, Dr. Xiaoyan Wang, Prof. Weiying Zheng, Dr. Xue Jiang, Dr. Yang Liu, Yana Fan, Prof. Zhigang Zhao, Dr. Changgeng Zhang, for their contributions to this benchmarking. The benchmarking researches were funded in part by the Natural Science Foundation of China, Hebei Natural Science Foundation, and Hebei Provincial Government's special fund for talent training. We are thankful for all comments and advice from computational electromagnetics colleagues worldwide. In particular, we are unfortunate that N. Takahashi, our great co-researcher, deceased young, and will always remember his cooperation and contribution to the establishment and development of the Problem 21 Family.

We sincerely thank Baobian research team, including Tao Liu, Linfeng Cai, Weiming Zhang, Meilin Lu, Junjie Zhang, and Fulai Che, for their cooperation in this benchmarking research. We also thank all graduate students from Hebei University of Technology, North China Electric Power University, including Yakun Tian, Yating Li, Yuezhi Cao, Yunlong Teng, and Junan Ji for their contributions in relevant numerical computation and experiments.

References

[1] Z. Cheng, Q.Hu, S. Gao, Z. Liu, C. Ye, M. Wu, J. Wang and H. Zhu, "An engineering-oriented loss model (Problem 21)," Proc. of the International TEAM Workshop, Miami, pp.137-143, 1993.

[2] S. Gao, M. Wu, H. He, J. Wang, Z. Liu, Q.Hu and Z. Cheng, "Problem 21$^+$: slotted non-magnetic steel plate driven by Problem 21's source," Proc. of the ICEF & TEAM Workshop, Yichang, pp.366-370, 1996.

[3] Z. Cheng, N. Takahashi, S. Gao and T. Sakura, "Loss analysis based on revised version of TEAM Problem 21," TEAM-Sapporo, 1999.

[4] N. Takahashi, T. Sakura, and Z. Cheng, "Nonlinear analysis of eddy current and hysteresis losses of 3-D stray field loss model (Problem 21)," *IEEE Trans. on Magn.*, vol.37, no.5, pp.3672-3675, 2001.

[5] N. Takahashi, K. Fujiwara and J. Takehara, "Basic study on characteristics of magnetic shielding and electromagnetic shielding," Software for Electrical Engineering Analysis and Design V (Edited: Wessex Institute of Technology), WIT Press, pp.79-86, 2001.

[6] Z. Cheng, N. Takahashi, Q.Hu and C. Fan, "TEAM-based benchmark family: Problem 21/21$^+$/21*," Proc. of the 4th IEE CEM, UK, 2002.

[7] Z. Cheng, R. Hao, N. Takahashi, Q.Hu and C. Fan, "Engineering-oriented benchmarking of Problem 21 family and experimental verification," *IEEE Trans. on Magn.,* vol. 40, no.2, pp.1394-1397, 2004.

[8] Z. Cheng, N. Takahashi, S. Yan, T. Asano, Q.Hu and X. Ren, "Proposal of Problem 21-based shielding model (Problem 21$^`$)," Proc. of TEAM Workshop, Shenyang, pp.15-20, 2005.

[9] Z. Cheng, N. Takahashi, S. Yang, T. Asano, Q. Hu, S. Gao, X. Ren, H. Yang, L. Liu, L. Gou, "Loss spectrum and electromagnetic behavior of problem 21 family", *IEEE Trans.on Magn*., vol.42, no.4, pp.1467-1470, 2006.

[10] Z. Cheng, N. Takahashi, S. Liu, S. Yang, C. Fan, Qi.Hu, L. Liu, M. Guo, and J. Zhang, "Benchmarking-based approach to engineering stray-field loss problems," presented at ACES-Miami, USA, 2006.

[11] Z. Cheng, N. Takahashi, S. Yang, C. Fan, M. Guo, L. Liu, J. Zhang and S. Gao, "Eddy current and loss analysis of multi-steel configuration and validation," *IEEE Trans. on Magn.,* vol.43, no.4, pp.1737-1740, 2007.

[12] Z. Cheng, N. Takahashi, B. Forghani, Y. Du, J. Zhang, L. Liu, Y. Fan, Q.Hu, C. Jiao, and J. Wang, " Large power transformer-based stray-field loss modeling and validation," Electric Machines and Drives Conference. IEEE International, pp.548-555 (Digital Object Identifier: 10.1109/IEMDC.2009.5075260), 2009.

[13] Z. Cheng, N. Takahashi, B. Forghani, G. Gilbert, J. Zhang, L. Liu, Y. Fan, X. Zhang, Y. Du, J. Wang, and C. Jiao, "Analysis and

measurements of iron loss and flux inside silicon steel laminations," *IEEE Trans. on Magn.,* vol.45, no.3, pp.1222-1225, 2009.

[14] Y. Du, Z. Cheng, B. Forghani, J. Zhang, L. Liu, Y. Fan, W. Wu, Z. Zhai and J. Wang, "Additional iron loss modeling inside silicon steel laminations," Electric Machines and Drives Conference. IEEE International, pp.826-831(Digital Object Identifier: 10.1109/IEMDC. 2009.5075299), 2009

[15] Z. Cheng, N. Takahashi, B. Forghani, G. Gilbert, Y. Du, Y. Fan, L. Liu, Z. Zhai, W. Wu, and J. Zhang, "Effect of excitation patterns on both iron loss and flux in solid and laminated steel configurations," (presented at Compumag-2009, Brazil) *IEEE Trans. on Magnetics*, vol.46, no.8, pp.3185-3188, 2010.

[16] Problem 21: 3-D Stray Field Loss Model: Benchmark Family(V.2009) available in electronic format at www.compumag.org/team.

[17] W. Zheng and Z. Cheng, "Efficient finite element simulation for GO silicon steel laminations using inner-constrained laminar separation," *IEEE Trans. on Magnetics*, vol.48, no.8, pp.2277-2283, 2012.

[18] Z .Cheng, N. Takahashi, B. Forghani, L. Liu, Y. Fan, T. Liu, J. Zhang, and X. Wang, "3-D finite element modeling and validation of power frequency multi-shielding effect," *IEEE Trans. on Magnetics***,** vol.48, no.2, pp.243-246, 2012.

[19] X. Wang, Z. Cheng, and L.Li, "Measurement and validation of stray loss based on improved TEAM Problem 21 Model," Trans. of Electrotechnical Society, Vol.28, no.6, pp.21-27, 2013.

[20] Z. Cheng, N. Takahashi, B. Forghani, X. Wang, et al, "Extended progress in TEAM Problem 21 family," COMPEL, 33, 1/2, pp.234-244, 2014.

[21] Z. Cheng, B. Forghani, X. Wang, L. Liu, T. Liu, Y. Fan, J. Zhang, X. Zhao, and Y. Liu, "Engineering-oriented investigation of magnetic property modeling and application," *International Journal of Applied Electromagnetics and Mechanics,* 55(2017), 147-158.

[22] X. Zhao, F. Meng, Z. Cheng, L. Liu, J. Zhang, and C. Fan, "Stray-field loss and flux distribution inside magnetic steel plate under harmonic excitation, COMPEL, 36, 6, pp. 1715–1728, 2017.

[23] X. Zhao, Y. Cao, Z. Cheng, B. Forghani, L. Liu, and J. Wang, "Experimental and Numerical Study on Stray Loss in Laminated Magnetic Shielding Under 3-D AC-DC Hybrid Excitations for HVDC Transformers," *IEEE ACCESS*. 2020.3014685/ *DOI*.10.1109.

[24] Z. Cheng，N. Takahashi, B. Forghani (eds), *Modeling and Application of Electromagnetic and Thermal Field in Electrical Engineering*(book), Science Press, Springer, 2020.